International Journal of Fluid Machinery and Systems
Vol. 8, No. 2, April-June 2015

DOI: 10.5293/IJFMS.2015.8.2.102
ISSN (Online): 1882-9554

Original Paper

Simulations of the Dynamic Load in a Francis Runner based on measurements of Grid Frequency Variations

Rakel Ellingsen[1], Pål-Tore Storli [1]

[1]Department of Energy and Process Engineering, Norwegian University of Science and Technology
Waterpower Laboratory, Alfred Getz vei 4, 7491 Trondheim, Norway, rakel.ellingsen@ntnu.no,
pal-tore.storli@ntnu.no

Abstract

In the Nordic grid, a trend observed the recent years is the increase in grid frequency variations, which means the frequency is outside the normal range (49.9-50.1 Hz) more often. Variations in the grid frequency leads to changes in the speed of rotation of all the turbines connected to the grid, since the speed of rotation is closely related to the grid frequency for synchronous generators. When the speed of rotation changes, this implies that the net torque acting on the rotating masses are changed, and the material of the turbine runners must withstand these changes in torque. Frequency variations thus leads to torque oscillations in the turbine, which become dynamical loads that the runner must be able to withstand. Several new Francis runners have recently experienced cracks in the runner blades due to fatigue, obviously due to the runner design not taking into account the actual loads on the runner. In this paper, the torque oscillations and dynamic loads due to the variations in grid frequency are simulated in a 1D MATLAB program, and measured grid frequency is used as input to the simulation program. The maximum increase and decrease in the grid frequency over a 440 seconds interval have been investigated, in addition to an extreme event where the frequency decreased far below the normal range within a few seconds. The dynamic loading originating from grid frequency variations is qualitatively found by a constructed variable T_{stress}, and for the simulations presented here the variations in T_{stress} are found to be around 3 % of the mean value, which is a relatively small dynamic load. The important thing to remember is that these dynamic loads come in addition to all other dynamic loads, like rotor-stator interaction and draft tube surges, and should be included in the design process, if not found to be negligible.

Keywords: Grid Frequency Variations, Torque Oscillations, 1D Simulations, Francis turbine, Dynamic loading

1. Introduction

The transition towards a more environmentally friendly society leads to a change in the way electricity is produced. Renewable energy sources like wind and solar energy are replacing the non-renewable sources like oil and gas, and this is good for the environment. Wind and sun energy are on the other hand much more unpredictable than oil and gas, since the access to the energy source varies a lot throughout the day. This makes it more difficult to match the production of electricity to the consumption.

Hydropower, on the other hand, has in many cases the opportunity to store water in reservoirs so the electricity can be produced when needed. The hydropower turbines may thus work as a form of battery, and this is beneficial for obtaining a balance between production and consumption. In addition, hydropower have short time scales for increasing and decreasing the power production, short time scales for start-up and shutdown and the possibilities for idle operation of pumped hydropower plants.

Several new and replacement high head Francis runners in Norway have broken down very quickly after installation over the last few years. The reasons for this are probably complex and uncertain, however it must be a natural conclusion that the runners were not properly designed for the operating condition and the dynamic loads where they were installed. Rotor-stator interactions (RSI), draft tube surges, oscillations in the hydraulic conduit system, planned changes in the power production, influences on the rotor from the generator and electrical system are all dynamic loads which needs to be accounted for in the design process for high head Francis turbines.

In this paper, the dynamic loads due to the frequency variations in the electrical grid are studied. Variations in grid frequency leads to variations in the speed of rotation of the runner since generators are synchronous machines. These variations in speed of

Received January 15 2015; revised May 1 2015; accepted for publication June 20 2015: Review conducted by Prof. Soon-Wook Kim. (Paper number O15029S)
Corresponding author: Pål-Yore Storli, Associate Professor, pal-tore.storli@ntnu.no

This paper was presented at the 27th IAHR Symposium on Hydraulic Machinery and Systems, September 4, Montreal, Canada.

rotation results in a dynamic load, which needs to be accounted for in the design process. The variations in the electrical grid frequency in the Nordic grid have increased over the last years, which means the frequency is outside the normal range (49.9-50.1 Hz) more often now than what was normal some years ago.

The rest of this chapter will focus on theory. First, the reason to why frequency variations occur is explained in section 1.2 and this is done by explaining how the electrical energy system and the primary governing work. The focus in section 1.2 is the increased frequency variations, and different explanations to why the variations have increased are given. Section 1.3 will explain how the frequency variations leads to torque oscillations and dynamic loading of the turbine.

1.1 Electrical energy system and primary governing

The electrical grid connects all the production units and the consumers through transmission lines. Since production of electricity is, in large, performed by synchronous generators, the grid frequency is proportional to the rotational speed of the producing units. In fact, the entire electrical energy grid is visualized in a good way as a huge mass, rotating at a rotational speed proportional to the momentary grid frequency. In this visualization, the power producing units are providing an accelerating torque to the rotating mass, and the power consumers are providing a decelerating torque. When these torques are equal, which means there is a balance between production and consumption of electricity, the frequency will be constant. If the torques are not equal, the frequency will change. As an example, decreased frequency means the consumption is higher than the production and if the total electricity production is not increased, the frequency will continue to decrease since the decelerating torque is bigger than the accelerating torque. Some mechanism to avoid this is needed since this clearly in undesirable.

Too big variations in the grid frequency might damage some of the components connected to the grid, and it is necessary to limit these variations. Limiting these variations imply rapidly matching production with consumption before the frequency has deviated too much. This is basically a task for the primary governing mechanism used in the electrical energy system. In the Nordic grid, a primary governing mechanism known as permanent speed droop is used. This mechanism is a part of the governors, and the mechanism increases the delivered power from each turbine when the grid frequency decreases, as illustrated in Fig. 1.

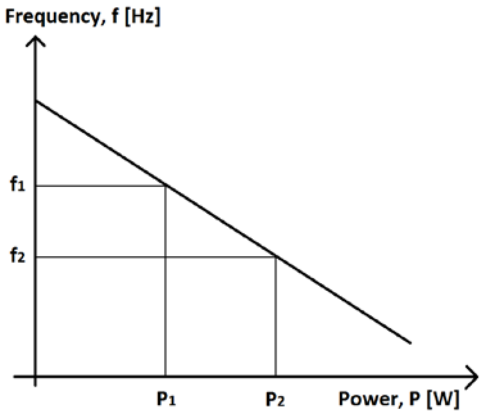

Fig. 1 Illustration of the permanent speed droop mechanism

When the grid frequency decreases from f_1 to f_2, the delivered power for a given turbine will increase from P_1 to P_2, and the slope of the curve in Fig. 1 decides how much the power changes with frequency. The slope is set in the governors and the steeper the curve is, the less will the given turbine contribute with primary governing [1]. The maximum slope of the curve is decided on by the Nordic Transmission System Operators (TSO).

Assuming that enough power plants (measured by installed power) are operating with speed droop characteristics, the frequency will stabilize when the production once again is equal to the consumption. This frequency will be different to the original frequency which means the speed droop mechanism allows for a frequency deviation from 50 Hz. This means that for the system to be stable the frequency must be allowed to deviate, since the primary governing is performed by the speed droop mechanism. The trend the resent years is an increase in frequency variations, and this has become such a worry that the Norwegian TSO has implemented a new secondary governing mechanism called Frequency Restoration Reserves (FRR) [2].

1.2 Variations in the grid frequency

Section 1.1 explained how an imbalance in production and consumption of electricity leads to changes in the grid frequency, and this section will focus on these variations in frequency. Figure 2 shows how the variations in the grid frequency in the Nordic countries have increased over the last years, represented by minutes outside the normal range (49.9-50.1 Hz) per week from 1996 to 2013 [2].

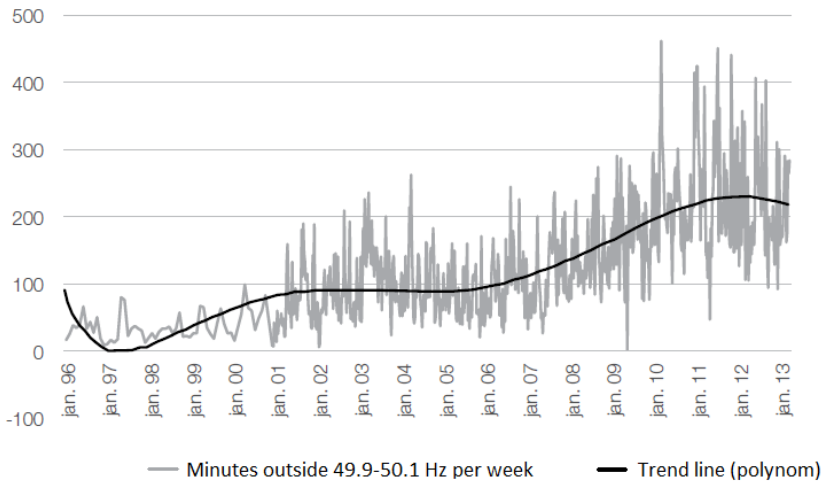

Fig. 2 Minutes where the grid frequency is outside the normal range of 49.9-50.1 Hz per week from 1996 to 2013 [2]

Two of the possible reasons for the increased variations seen in Fig. 2, are utilization of new non-regulated energy sources, and the fact that the generation schedule is made with hourly steps [2] [3]. The problem with non-regulated energy resources like wind and sun is the unpredictable access to the energy, which means the synchronous machines with permanent speed droop must work even harder to balance the production to consumption. The hourly steps in generation schedule is due to an hourly spot market, where the power output from the generators are changed maximum once an hour according to the forecast of demand for electric power. If the demand is exactly as the hourly planned production, meaning the same as the set points on the units, the frequency will be 50Hz. Deviations from the production plan will then create deviations in the frequency as the production and consumption will find a new equilibrium at a different frequency via the permanent speed droop mechanism. Figure 3 shows the frequency variations over 24 hours, and the peaks seen once an hour represents the problem with a generation schedule with hourly steps.

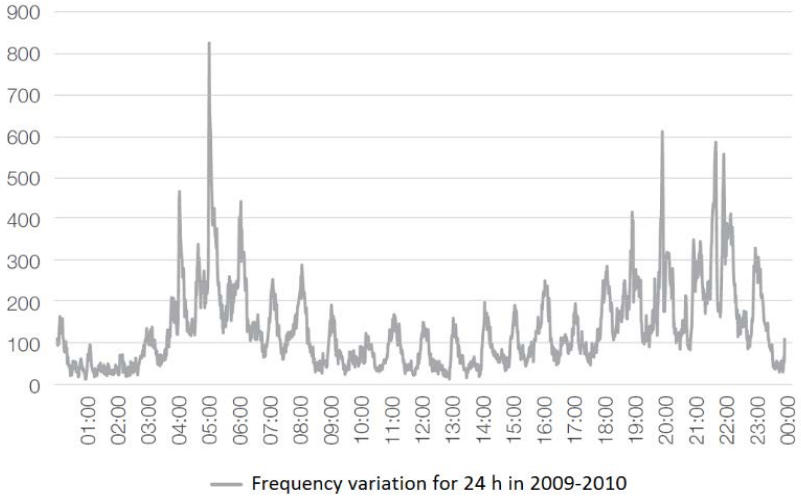

Fig. 3 The variations in the grid frequency over 24 hours represented by the number of events outside the 49.9-50.1 Hz range per minute in the years 2009-2010 [2]

The rotating ineria from runners and generators contributes to stabilize the grid frequency, because the rotating inertia absorb or provide a lot of energy when the turbines change their rotational speed. This means more energy is needed in order to change the state of the system for electrical grids were the rotating masses are big [2]. Europe have many thermal power plants, and these power plants do usually have high amounts of rotating inertia. Norway's electricity production consists mostly of hydro power plants, and hydro turbines do often have smaller inertia compared to the thermal power plants, meaning their rotating masses will contribute less in keeping the frequency stable. This might explain why the frequency tends to vary more in the Nordic countries than in rest of Europe. In addition, the number of production units is much bigger in central Europe, which makes the frequency deviate less in Central Europe than in the Nordic countries when a big production unit loose contact with the grid.

Some factors might have contributed to a reduction in the rotating inertia in the Nordic countries over the last years, and this might partly explain the increasing trend in Fig. 2. One of these factors is the implementation of small hydro power plants, because these power plants do not contribute much with system inertia [2]. Wind turbines have also been implemented, and they do usually not contribute system inertia at all, because they are connected with frequency converters [2]. The increased import of electricity through high voltage direct current cables is a third factor, which also reduces the system inertia and thus the frequency

stability.

Another possible reason for increased frequency deviations at the consumer end might be that almost all new household appliances use power electronics, while old appliances used transformers which reduced the load with decreasing frequency. It has been suggested that this transition leads to more unstable grid frequency since the newer appliances do not contribute to the grid stabilization while the old appliances did. This is because the transformer contributes to grid stabilization by reducing power flow at reduced frequency, thus giving an intrinsic load reducing property to the consumer end of the system.

The speed droop, as explained in section 1.1, is a part of the primary governing mechanism. An automatic secondary governing market was introduced in the Nordic countries in 2013 in addition to the primary- and tertiary markets, and this is assumed to account for the decrease in the trend from 2013 in Fig. 2 [2]. The tertiary market is today controlled manually, unlike the primary and secondary market, and the tertiary market reduces regional bottlenecks and frees the primary and secondary reserves [2].

1.3 Torque oscillations and dynamic loading

The focus in the previous section was the frequency variations and why these variations have increased over the last years. This section will explain what will happen to the torques in the turbine when exposed to frequency variations.

The turbine runner and generator rotor are connected to the same shaft and are rotating in the same direction. The hydraulic torque T_h from the water acting on the runner will try to accelerate the turbine, while the magnetic torque T_m acting on the generator will try to decelerate the turbine, see Fig. 4.

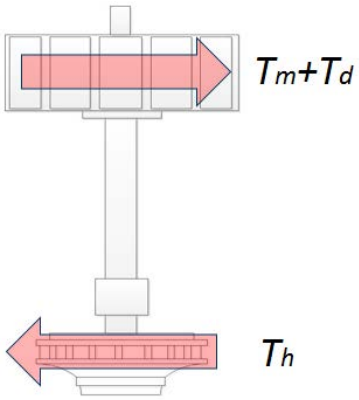

Fig. 4 Torque in runner (T_h) and generator (T_m and T_d)

T_d in Fig. 4 is the dampening torque from a mechanism in the generator, and can work both as accelerating and decelerating torque.

T_m, T_d and T_h can be summarized with Newton's second law, and the result is seen in eq. (1)

$$J\frac{d\omega}{dt} = \sum T = T_h - T_m - T_d \tag{1}$$

J is here the mass moment of inertia, ω is the angular velocity of the runner, and T is torque. If the summation of the torques are zero, the speed of rotation is constant, while unequal torques will lead to a change in the speed of rotation according to eq. (1). When the accelerating torques are larger than the decelerating torques, the angular velocity will increase according to eq. (1), and vice versa when the decelerating torques are the largest.

The grid frequency is determining how fast the generator stator magnetic field is rotating. When generating power, the magnetic field of the rotor is pulling on the magnetic field of the stator, and these fields are separated in phase by the magnetic torque angle δ. The magnitude of δ is directly linked to the torque acting on the rotor from the stator (T_m) as eq. (2) shows.

$$T_m = T_{nom}\frac{\sin\delta}{\sin\delta_{nom}} \tag{2}$$

T_{nom} in eq. (1) is the nominal torque and δ_{nom} the nominal torque angle. If the grid frequency increases, the stator magnetic field is catching up to the rotor field, meaning δ and thus the torque acting on the rotor from the stator is decreased.

Variations in grid frequency will lead to variations in δ, and generators are often equipped with some sort of dampening mechanism which dampens these variations, see T_d in eq. (3) [4].

$$T_d = m_d\frac{d\delta}{dt} \tag{3}$$

m_d is a constant. The damping torque will counteract the change in torque angle, and can work both as accelerating and decelerating torque.

The hydraulic torque T_h is a function of the hydraulic power, P_h, and ω, see eq. (4).

$$T_h = \frac{P_h}{\omega} = \frac{\rho g Q H \eta_h}{\omega} \tag{4}$$

P_h depends on head, H, and volume flow, Q, and the guide vanes are adjusted in order to make sure the delivered power from the turbine corresponds to the demand. ρ in eq.(3) is water density, g is the gravitational constant and η_h is the hydraulic efficiency.

A change in the grid frequency will lead to changes in both ω and T_h in eq. (3). ω changes with frequency because the generators are synchronous machines, while T_h changes because the permanent speed droop counteracts the frequency variation, as already explained in section 1.1. For example, a decrease in frequency means ω decreases, which will reduce T_h according to eq. (3). The permanent speed droop in the governor will counteract the frequency decrease by opening the guide vane so Q and P_h increases, and this will reduce T_h even further. The speed droop mechanism will thus amplify the changes in T_h because of frequency variations, and this is the main reason to why the speed droop mechanism is included in the simulations.

If T_h increases while T_m is held constant, the speed of rotation will increase as a result, according to eq. (4). This means the generator rotor will rotate faster than the magnetic field in the stator, which is given by the grid frequency. δ will then increase, and so will the induced torque in the generator until the magnitudes of the hydraulic torque and the induced torque are equal again [5].

An increase in the grid frequency leads to increased rotational speed of the magnetic field in the stator in the generator. This means δ is reduced, which reduces the magnetic torque and thus the decelerating torque [4]. The speed of rotation of the turbine will then increase until the torques are equal and the grid frequency are once again proportional to the speed of rotation of the turbine.

The rotor can be visualized as a giant torsion bar, where the torques acting on each end leads to tensions. This visualization is similar to a spring for linear motion, and it is the basis for a qualitative measure of dynamic loading. Equation (4) is zero for steady state operation, but this is not the case for the dynamic loading of the runner. A different qualitative measure of the dynamic loading is therefore constructed, and the parameter T_{stress} is chosen here, see eq. (5).

$$T_{stress} = \frac{T_h + T_m}{2} + T_d \tag{5}$$

T_{stress} is not a physical property, but it is convenient to use as a measure of dynamic loading. T_d is zero at steady state operation according to eq. (3). This makes T_{stress} equal to the average of T_h and T_m for steady state operation, which makes sense because T_h and T_m must then be equal in magnitude and opposite in direction and T_{stress} will be equal to the average between the two torques.

2. Methodology

In order to quantify the dynamic loading on a hydro turbine rotor, it was necessary to do simulations, as actual measurements of stress in a runner were not possible in the limited time available. However, other measurements at a hydropower plant were performed, and some of these measurements were used as input to the simulations or to compare simulations to. This chapter presents the methodology, and it includes both the measurements at the hydropower plant and the simulations.

2.1 Measurements at a hydropower plant

The measurements were carried out at Grana hydropower plant, and the layout is seen in Fig. 5.

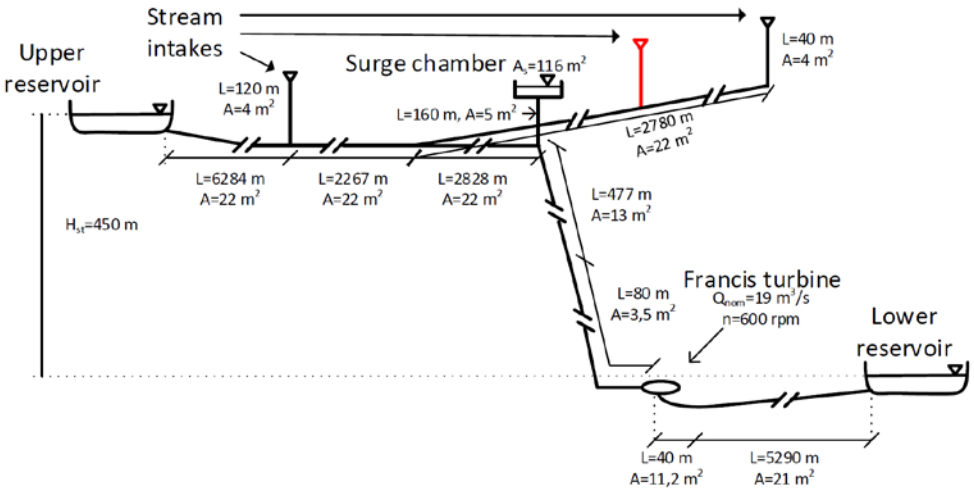

Fig. 5 The layout of the hydropower plant Grana. The stream intake in red is omitted from the simulations

The grid frequency was one of the measured parameters, and these measurements were performed by the use of a National Instrument (NI) module, which counted cycles per second directly on the 230 V main. These measurements did not need any calibration, and the measurements are highly accurate, which is important because the measurements are used as input to the simulations.

In addition to the grid frequency, the speed of rotation, guide vane opening and delivered power from the generator were also measured at the power plant. These measurements are not used as input to the simulations, and they are only used for comparison with simulated results and to record load variations. The three measurements (not included the grid frequency) use some of the equipment already installed at the power plant. In order to record and log the data from the measuring equipment, a resistance of 500 Ω is inserted in the 0-10 mA measuring loop so the voltage over the resistance is in a suitable range for a -5.0 V - 5.0 V NI logging device. The measured voltage values are then manipulated so they better represent the measured quantities. These measurements are not as precise as the frequency measurements, but the measurements are good enough to see if there are any changes in the measured parameters.

LabVIEW has been used for logging and averaging of data, and the logging frequency was set to 250 Hz. The values were averaged over one second and then written to file.

The measurements were performed from October 2013 to January 2014, but the turbine was only operational for the last month.

2.2 1D Simulations with measured frequency as input

The frequency measurements were analyzed in order to find interesting events to investigate in the simulation program. Both the maximum increase and decrease in grid frequency over a given time interval was chosen, since these events lead to the biggest torque oscillations. The maximum increase and decrease in frequency within an interval of 500 seconds was studied in [4], and in this paper the interval is set to 440 seconds. A case where the frequency decreased far below the normal range within a few seconds is also simulated, and this happening is from now on referred to as the extreme case.

The simulations are performed using an in-house 1D simulation program made in MATLAB utilizing the Method of characteristics (MOC) for the pipes and hydraulic conduits. MOC makes the model fully elastic. For the turbine runner, a turbine model developed by Torbjørn K. Nielsen is used [6]. The turbine model includes both the speed of rotation, volume flow through the runner and head. In the simulations, these three variables needs to be solved, as well as the electric current, voltage, magnetic flux, torque angle and a simple voltage governor representing the generator. A PI-governor is used, and the permanent speed droop mechanism is included. These seven variables are solved using Newton's method and Euler integration.

The measured grid frequency for the three chosen frequency events, are used as input to the simulations. The goal with the simulations is to investigate how these frequency variations influences the turbine, and in order to do this, both the conduit system surrounding the turbine, runner, generator and governor needs to be modeled. Figure 5 presented the power plant with reservoirs, stream intakes, surge chamber and a Francis turbine. The red stream intake in Fig. 5 is omitted from the simulations.

The results from the seven variables which was evaluated in the simulation program are further investigated by the use of eq. (2), (3) and (4) for the magnetic torque, the dampening torque and the hydraulic torque respectively. Neither the measurements at the power plant, nor the simulations involve the stresses in the material in the runner. A qualitative measurement of the dynamic loading is thus necessary in order to connect the simulated torques to the dynamic loading in the material. T_{stress} from eq. (5) was used for this purpose, and T_{stress} is calculated in MATLAB.

3. Results

This chapter will present the results from the simulations and measurements, starting with the results from the case where the frequency decreased most within the 440 seconds time interval in section 3.1. Next, section 3.2 shows the results from the simulations where the frequency increased most within the same time interval. Section 3.3 will then present the results from the extreme case. In section 3.4 two comparisons between the measurement and the simulations are presented.

The results are presented graphically with time on the abscissa and the variable on the ordinate. All simulations starts 200 seconds before the studied frequency event. In the figures in sections 3.1 and 3.2, the first 200 seconds are omitted, meaning the presented time interval of 440 seconds (from 200 s to 640 s) only shows results for the chosen frequency event. The figures in section 3.3 start at zero, and the 200 first seconds are from before the studied frequency event.

A presentation of the simulated grid frequency over the time interval is given in the three first subchapters. Sections 3.1 and 3.2 presents how the normalized values for the guide vane opening κ, power delivered from the generator P_{el} and the angular velocity ω varies with time, and sections 3.1, 3.2 and 3.3 presents how the normalized value for T_{stress} varies with time. Section 3.4 presents comparisons for κ, P_{el} and ω for the case where the frequency is increasing and for the extreme case.

3.1 Decreasing grid frequency

This section presents the results from the case where the frequency decreased most within the 440 s interval, and this frequency event is from right after 2:00 the 24th of December 2013. First, the measured grid frequency is presented in Fig. 6.

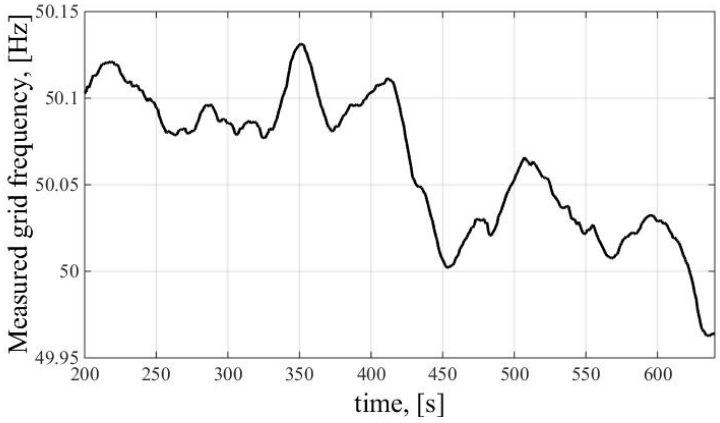

Fig. 6 The measured grid frequency for the case where the frequency is decreasing

Figure 6 shows that the maximum change in grid frequency is approximately 0.17 Hz over the 440 s period. The biggest continuous drop in frequency is from 50.11 Hz to 50 Hz, and the grid frequency is outside the 49.9-50.1 Hz range approximately 90 seconds out of 440 seconds.

Figure 7 presents the normalized values for ω, P_{el}, and κ, and Fig. 8 presents the normalized value for T_{stress}.

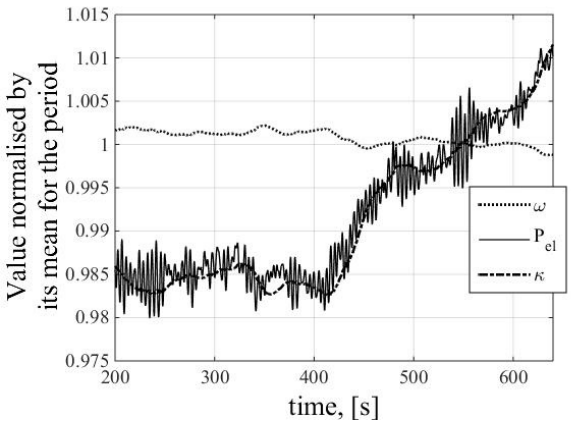

Fig. 7 Normalized values for ω, P_{el} and κ for the case where the frequency is decreasing

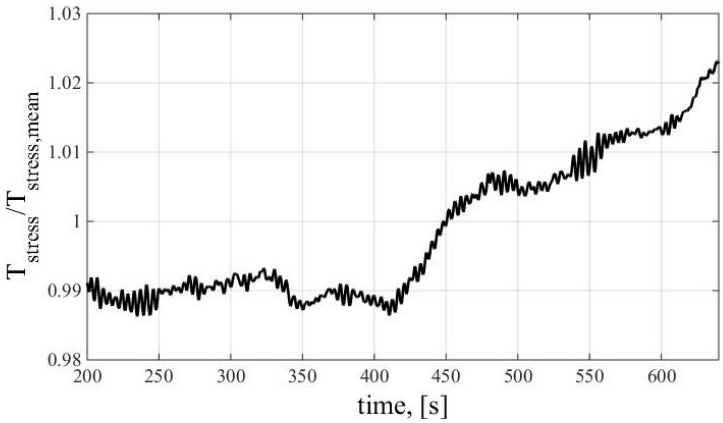

Fig. 8 Normalized values for T_{stress} in the case where the frequency is decreasing

Figure 7 shows that the change in P_{el} and κ is approximately 2.6 % of the mean value, while the change in ω is approximately 0.3 % of the mean value. Figure 8 shows that the changes in T_{stress} is over 3 % of the mean value.

3.2 Increasing grid frequency

This section presents the results from the case where the frequency increased most within the 440 s interval, and this frequency event is from approximately 9:15 the 24th of December 2013. First, the measured grid frequency is presented in Fig. 9.

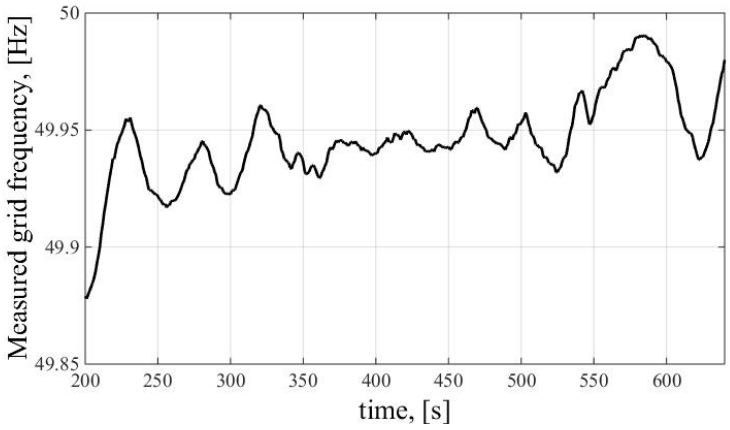

Fig. 9 The measured grid frequency for the case where the frequency is increasing

Figure 9 shows that the maximum change in grid frequency is approximately 0.11 Hz over the 440 s period. The interval where the frequency continuously increases the most is found within the 30 first seconds where the frequency increases from 49.88 Hz to 49.96 Hz. The frequency in Fig. 9 is outside the 49.9-50.1 Hz range for only 10 seconds out of 440 seconds.

Figure 10 presents the normalized values for ω, P_{el}, and κ, and Fig. 11 presents the normalized value for T_{stress}.

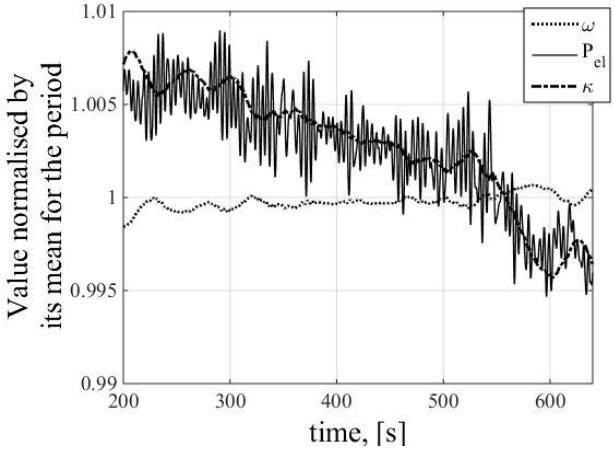

Fig. 10 Normalized values for ω, P_{el} and κ for the case where the frequency is decreasing

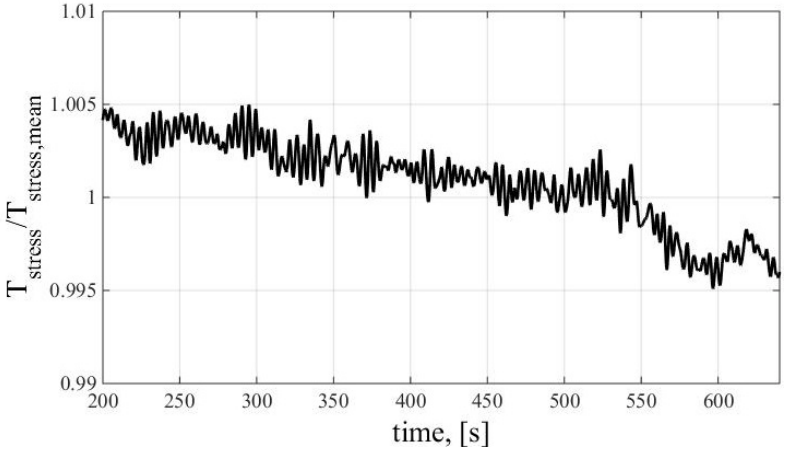

Fig. 11 Normalized values for T_{stress} in the case where the frequency is decreasing

Figure 10 shows that the changes in P_{el} and κ is approximately 1 % of the mean value, while the change in ω is approximately constant. Figure 11 shows that the change in T_{stress} is approximately 1 % of the mean value.

3.3 Extreme case

This section presents the results from the extreme case, and this frequency event is from right after 8:00 the 20th of December 2013. Figure 12 presents the measured grid frequency for the extreme case, and Fig. 13 presents the normalized values for T_{stress}.

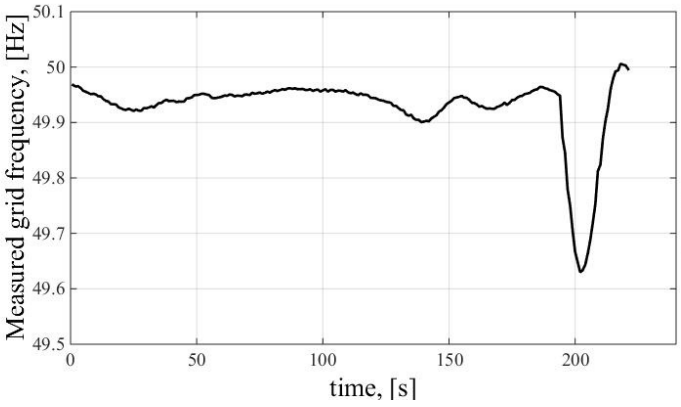

Fig. 12 The measured grid frequency for the extreme case

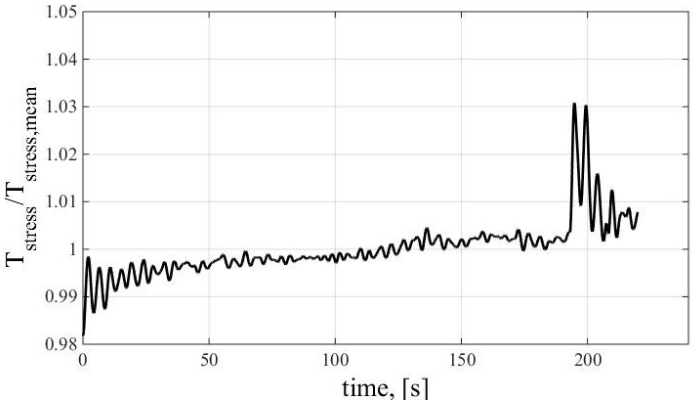

Fig. 13 Normalized values for T_{stress} for the extreme case

The grid frequency for the extreme case is outside the normal range for only 17 seconds, and the frequency is 49.63 Hz at the lowest. Figure 13 shows that the jump in T_{stress} is approximately 3 % of the mean value.

3.4 Comparison with measurements from the power plant

This section will present two comparisons between simulations and measurements in order to see if the results from the simulation program are equal to the measurements from the power plant. Figure 14 presents a comparison for κ, P_{el}, and ω for the case where the frequency is increasing, and Fig. 15 presents the same kind of comparison for the extreme case. The comparison for the case where the frequency is decreasing is not included here.

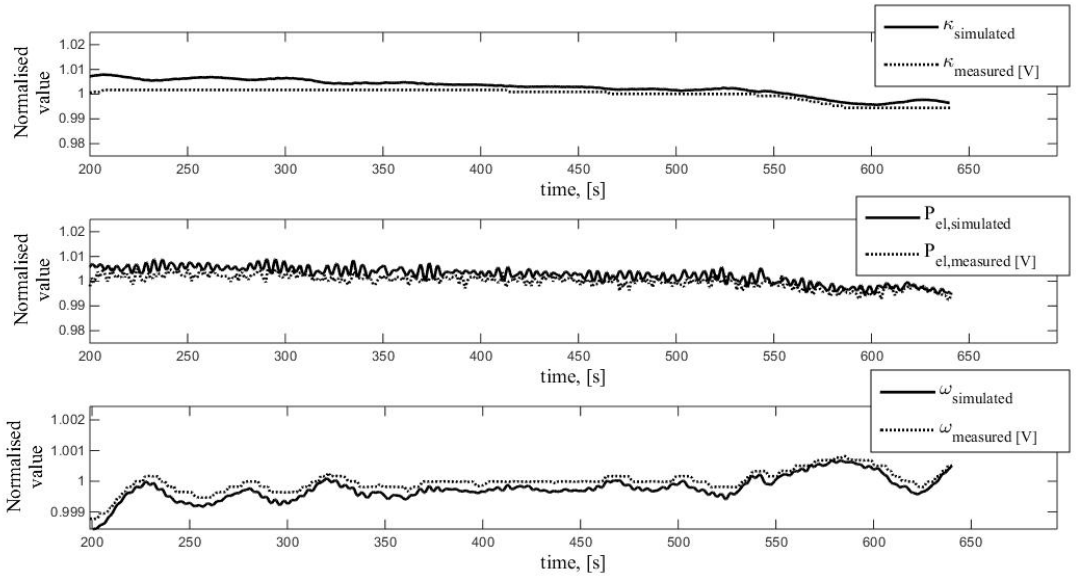

Fig. 14 Comparison of simulations and measurements for κ, P_{el} and ω for the case where the frequency is increasing

The simulations are corresponding well to the measurements for all three variables in Fig. 14.

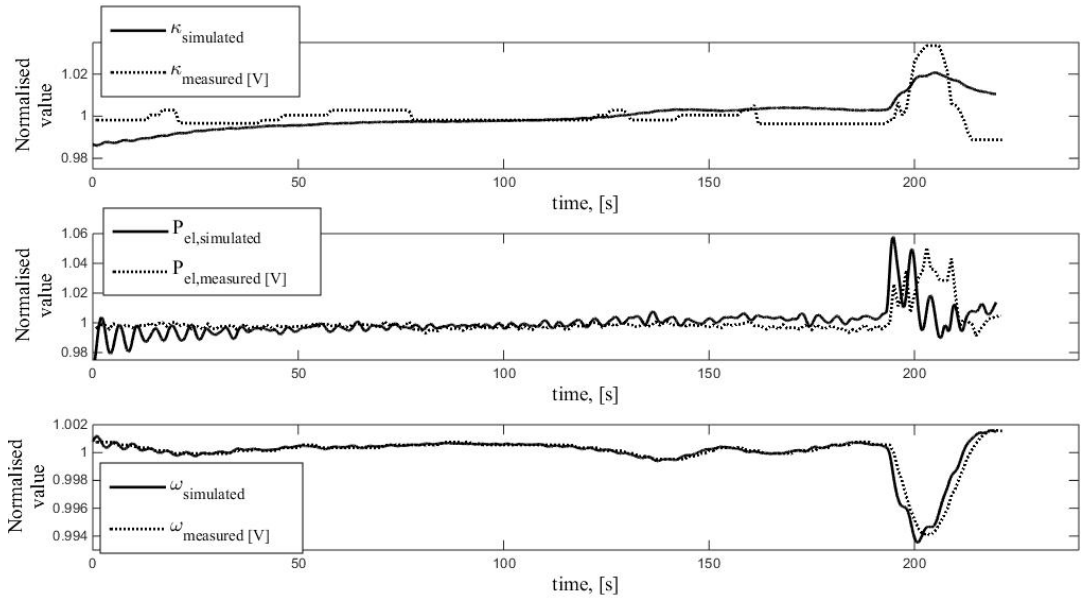

Fig. 15 Comparison of simulations and measurements for κ, P_{el} and ω for the extreme case

The simulations do not correspond very well to the measurements for κ, and P_{el}, and especially not after the frequency decrease at 200 s. The simulations for ω does on the other hand show very good results both before and after 200 s.

4. Discussion

The previous section presented some results from both measurements and simulations, and the results from section 3.1, 3.2 and 3.3 are discussed in section 4.1. Section 4.2 will discuss the results from the comparisons presented in section 3.4.

4.1 Simulations

Figures 6 and 9 presented the grid frequency for the case with maximum decrease and increase within the 440 s interval respectively. The variations in frequency are not very big for neither of these two events, and the case where the frequency is decreasing have the biggest frequency variation. When comparing figures 7 and 8 to figures 10 and 11, it is clear that the changes in ω, P_{el}, κ, and T_{stress} were bigger for the case where the frequency decreased. This is expected since the frequency variations were bigger in this case. The measured frequency is inside the 49.9-50.1 Hz range for both cases most of the time.

The grid frequency for the extreme case was presented in Fig. 12, and the lowest frequency in this figure is 49.63 Hz. This is below the normal range (49.9-50.1 Hz), but 49.63 Hz is above the lower limit of 49.5 Hz, which is accepted as a transient frequency deviation, occurring for instance when a big production unit suddenly lose its connection to the grid [2]. The time constant for hydropower plants is approximately 6 seconds, which means it will take less than 10 seconds for the system to discover the drop in frequency and compensate by delivering more power. The frequency in Fig. 12 recovers after a few seconds, which is not surprisingly when the time constant is taking into account.

ω seem to follow the grid frequency, and this is seen by comparing the ω curve in Fig. 7 with the frequency curve in Fig. 6, and the ω curve in Fig. 10 with the frequency curves in Fig. 9. It is only possible to compare the shape of these curves and not the actual value since ω is normalized by its mean value while the frequency is the measured frequency. The corresponding curves are no surprise because ω strongly depends on the measured frequency.

The curves for P_{el}, κ and T_{stress} are very similar to each other in shape, and this makes sense because the produced power is closely connected to the amounts of water going through the runner, which depends on κ.

Both P_{el} and T_{stress} in figures 7, 8, 10 and 11 shows oscillations, and this is assumed to be because of the oscillations in δ.

T_{stress} for the case with decreasing frequency changes with over 3 %, but for the case with increasing frequency, T_{stress} only decreases with 1 %. In the extreme case, T_{stress} increases with 3 % in one jump. When comparing T_{stress} in Fig. 13, which is for the extreme case, with T_{stress} in Fig. 8 for the case with decreasing frequency, it is possible to see that the jump in T_{stress} is bigger in the extreme case. The overall increase in T_{stress} over the 440 s interval is in the same magnitude as the instantaneous increase in T_{stress} in the extreme case. In a previous work where the max and min frequency deviations for 500 seconds for the entire measurement period was used, the variations for T_{stress} were found to be much higher [4].

4.2 Comparison with measurements from the power plant

In general, the simulated values are closer to the measured values for the case where the frequency is increasing. This is assumed to be because the frequency variations are smaller and slower for the case where the frequency increases than for the extreme case. It is then easier for both power plant and simulation program to follow the changes.

In Fig. 15 it is possible to see a step wise variation in $\kappa_{measreud}$, while $\kappa_{simulated}$ changes more smoothly. This is assumed to be because the measurements at the power plant are quite simple and crude, and may thus lead to a discrete presentation of the measured parameter.

$P_{el,simulated}$ corresponds relatively well to $P_{el,measured}$ in Fig. 14. In Fig. 15, $P_{el,simulated}$ is not equal to $P_{el,measured}$ after the decrease in frequency occurred after 200 s. The simulation program might thus not be as good when the changes in frequency are too big, and in order to capture swift and large changes, a more refined model for the generator and it's governor are needed.

The simulations for the angular velocity ω shows best coherency to the measured value**,** and this is easiest to see in Fig. 15. It is not surprising since both $\omega_{simulated}$ and $\omega_{measured}$ are closely connected to the measured frequency. The simulated angular velocity was the variable who corresponded best to the measurements in a previous work [4].

5. Conclusion

The dynamic loading originating from grid frequency variations is qualitatively found by a constructed variable T_{stress}. For the simulations presented here, the variations in T_{stress} are found to be around 3 % of the mean value, which is a relatively small dynamic load. Previous work found the variations in T_{stress} to be between 4% and 6 % [4]. The important thing to remember is that these dynamic loads come in addition to all other dynamic loads, like RSI and draft tube surges, and should be included in the design process, if not found to be negligible. Several new Francis runners in Norway have broken down the last years, and it must be a natural conclusion that they were not properly designed for the actual loads they experienced. Since no-one intentionally designs a runner that would fail, there must be something that is fundamentally not understood or taken into account in the design process. We are not claiming that the missing link to predicting runner failure is the variations in grid frequency, but it is something that should be further investigated. Knowing that the more dangerous dynamic loads are when the mean stress in the material is high, and that the mean stress also is higher when the speed of rotation is low, attention towards dynamic loads at high load operation and low grid frequency could provide new knowledge that would change design criteria, and thereby hopefully avoiding new runner failures.

6. Further Work

The topic will be further investigated, and the next steps are likely to involve simulations were both Computational Fluid Dynamics (CFD) and Finite Element Method (FEM) on a turbine runner are combined. It is then possible to simulate how the frequency variations impacts the local stresses in the material in the turbine runner. The results from these simulations will be a better measurement for the dynamic loading than the qualitative measurement T_{stress} used here. If the variations in the stresses are big enough, they might contribute to a shortening of the fatigue life of the runner. In addition to the CFD and FEM simulations, experiments on a model runner might be conducted. Model runners are usually very stiff, and the idea is to construct a more flexible runner so the movements in the material due to the frequency variations are big enough to detect with strain gauges. This will make it possible to compare the results from the simulations with measurements.

Nomenclature

A	Cross-sectional area [m^2]
L	Length of pipes [m]
g	Gravitational constant [ms^{-2}]
H	Head [m]
J	Mass moment of inertia
m_d	Constant
P	Power [W]
Q	Volume flow [m^3/s]
T	Torque [Nm]
t	Time [s]

Greek symbols

δ	Torque angle
η	Efficiency
κ	Guide vane opening
ρ	Fluid Density [kg/m^3]
ω	Angular velocity [rad/s]

Subscripts

d	Dampening
el	Electrical, from generator
h	Hydraulic
m	Magnetic
nom	Nominal
$stress$	Stress, qualitative measure for stress
st	Static
s	Surge Shaft

References

[1] Nielsen, T. K. and Storli, P.-T. 2014, “Measurements and simulations of turbines on a common grid”, IOP Conference Series: Earth and Environmental Science, Vol. 22

[2] Statnett, 2014, “Systemdrifts- og Markedsutviklingsplan 2014-2020. Tiltaksplan for sikker og effektiv drift av krafverksystsemet”

[3] Eurelectric and Entso-E, 2011,”Deterministic frequency deviations – root causes and proposals for potential solutions”, A joint EURELECTRIC – ENTSO-E response paper

[4] Storli, P.-T. and Nielsen, T.K., 2014, “Dynamic load on a Francis turbine runner from simulations based on measurements”, IOP Conference Series: Earth and Environmental Science, Vol. 22

[5] Chapman, S., 2005, Electric Machinery Fundamentals, McGraw-Hill Companies, Incorporated

[6] Nielsen, T. K., 1996, “Dynamic Behaviour of Governing Turbines Sharing the Same Electrical Grid”, 18th IAHR Symposium on Hydraulic Machinery and Cavitation, Valencia, Kluwer Academic Publisher